https://doi.org/10.5194/gmd-2021-20
Preprint. Discussion started: 29 March 2021

Geoscientific Model Development Discussions

A Lagrangian-based Floating Macroalgal Growth and Drift Model (FMGDM v1.0): application in the green tides of the Yellow Sea

Fucang Zhou[1], Jianzhong Ge[1,2], Dongyan Liu[1,2], Pingxing Ding[1,2], Changsheng Chen[3]

[1]State Key Laboratory of Estuarine and Coastal Research, East China Normal University, Shanghai, 200241, China
[2]Institute of Eco-Chongming, No.20 Cuiniao Road, Chenjiazhen, Shanghai 202162, China
[3]School for Marine Science and Technology, University of Massachusetts-Dartmouth, New Bedford, MA 02744, United states

Correspondence to: Jianzhong Ge (jzge@sklec.ecnu.edu.cn)

Abstract. Massive floating macroalgal blooms in the ocean have had an array of ecological consequences; thus, tracking their drifting pattern and predicting their biomass are important for their effective management. However, a high-resolution ecological dynamics model is lacking. In this study, a physical–ecological model, Floating Macroalgal Growth and Drift Model (FMGDM v1.0), was developed to determine the dynamic growth and drift pattern of floating macroalgal, based on the tracking, replication and extinction of Lagrangian particles. The position, velocity, quantity and represented biomass of particles are updated synchronously between the tracking module and the ecological module. The former is driven by ocean flows and sea surface wind, while the latter is controlled by the temperature, salinity, and irradiation. Based on the hydrodynamic models of the Finite-Volume Community Ocean Model and parameterized using a culture experiment of *Ulva prolifera*, which caused the largest bloom worldwide of the green tide in the Yellow Sea, China, this model was applied to simulate the green tides around the Yellow Sea in 2014 and 2015. The simulation result, distribution and biomass of green tides, was validated using remote sensing observation data and reasonably modeled the entire process of green tide bloom and its extinction from early spring to late summer. Given the prescribed spatial initialization from remote sensing observation, the model could provide accurate short-term (7–8 d) predictions of the spatial and temporal developments of the green tide. With the support of the hydrodynamic model and biological data of macroalgae, this model can forecast floating macroalgae blooms in other regions.

1 Introduction

Floating macroalgae, primarily brown algae and some green algae, occurs extensively in oceans. Except some entirely pelagic species, like *Sargassum*, most floating macroalgae grow in the intertidal zone during their early life stages (Rothäusler et al., 2012). Massive floating macroalgal blooms have frequently recurred in many coastal regions worldwide (Smetacek and Zingone, 2013) and had deleterious effects on economic activities and ecosystems of the affected coastal areas (Lyons et al., 2014; Teichberg et al., 2010).

Some floating macroalgae blooms are seasonal, such as the *Sargassum* originating from the Gulf of Mexico and the green tide in the Yellow Sea, China (YS) (Gower and King, 2011; Liu et al., 2009). Under suitable temperature and solar radiation, the blooms primarily begin in the spring every year, are advected into the adjacent sea, and grow rapidly in the subsequent floating life stages until they die. The biomass of floating green tide in YS can exceed one million tons in late June (Liu et al., 2013; Song et al., 2015). A few techniques have been used to detect the blooming process of floating macroalgae, such as field and remote sensing observations. However, field observations exhibit site-limitation and are costly. Moreover, determining the overall spatial development of macroalgae blooms in the entire regional sea is difficult (Liu et al., 2015). Remote sensing techniques can effectively estimate the coverage and quantify the total biomass (Hu et al., 2019; Wang and Hu, 2016), but they cannot observe the entire process owing to technical limitations and cloud cover (Keesing et al., 2011). Timely assessment and accurate prediction of coverage and biomass are very important for the management and prevention of floating macroalgae bloom.

https://doi.org/10.5194/gmd-2021-20
Preprint. Discussion started: 29 March 2021

Geoscientific Model Development Discussions

Numerical simulation is one of the most cost-effective methods of forecasting spatiotemporal variations of locations and biomass for floating macroalgae. Based on the hydrodynamic numerical model, the drift trajectory of floating macroalgae can be determined (Lee et al., 2011; Putman et al., 2018). The biogeochemical and ecosystem numerical models for macroalgae growth are also widely applied in the study of estuaries and coasts (Lovato et al., 2013; Perrot et al., 2014; Sun et al., 2020). The biomass, growth, and spatial coverage of the floating macroalgae change dynamically over time. The growth and mortality are controlled by changing environmental factors, such as temperature, light intensity, salinity, dissolved nutrients, dissolved oxygen, seawater turbidity, and predation by zooplankton (Cui et al., 2015; Shi et al., 2015; Xiao et al., 2016). Incorporating physical drifting models and the biogeochemical growth model appears to be essential to high-precision simulation (Brooks et al., 2018). However, the temporal variation of biomass could not be determined via physical modeling; meanwhile, the ecological growth model failed to predict the spatial transportation of floating macroalgae. The efficient management and forecasting of massive floating macroalgal blooms were limited by the lack of high-precision coupled physical drift prediction models and ecological dynamics models to predict spatiotemporal variations of floating locations and biomass (Wang et al., 2018).

In this study, a physical–ecological coupled growth and drift model of floating macroalgal was developed, and the influence of environmental factors such as temperature, light intensity, and salinity was considered for the ecological module. Based on the regional ocean numerical model system and sufficient physiological data, the drift and growth process of different floating macroalgae blooms can be determined and predicted using FMGDM. Based on the Finite-Volume Community Ocean Model (FVCOM), this coupled model was applied to the recurrent green tide of YS. By setting up the model based on the data of the physiological and bloom pattern of *U.prolifera* green tide in YS, the blooming process in the summer of 2014 and 2015 was simulated in this study, and the result, which was compared with satellite data and biomass estimation data, indicated that the model was robust.

The rest of this paper is organized as follows. In Section 2, the development of FMGDM v1.0, data sources and the research method of green tide in YS are described. In Section 3, this coupled model is applied to the green tides of YS. The role of physical driving factors is discussed, and the full processes of green tides bloomed in the YS in 2014 and 2015 are simulated and verified using satellite data. In Section 4, the uncertainties and prospects of FMGDM development and application are discussed. Major innovations of this model are summarized, and the future outlooks of this model o are proposed in Section 5.

2 Methodology

2.1 Model framework

The model system for floating macroalgae growth and drift (FMGDM v1.0) consisted of a Lagrangian particle tracking module and an ecological module for macroalgae growth and mortality (Fig. 1). The floating drift process is described by the Lagrangian tracking module, which is developed based on the FVCOM v4.3 offline Lagrangian tracking model (http://fvcom.smast.umassd.edu/), and driven by surface wind and ocean flows. By contrast, in the macroalgae ecological module, the dynamic growth and mortality process in the floating state are exhibited by particle replication and disappearance, and the daily growth or mortality rate of each simulated particle is determined dynamically by the temperature, salinity, and irradiation where the floating particle is in space and time. The position, velocity, quantity and represented biomass of particles are updated synchronously between two modules. All the forcing fields and environmental forcing are updated from the regional and local weather and ocean numerical model system. Based on the update of simulated particles in spatial and biomass, the coupled tracking and ecological model, which is applicable in the coverage and biomass simulation of floating macroalgae, is achieved.

https://doi.org/10.5194/gmd-2021-20
Preprint. Discussion started: 29 March 2021

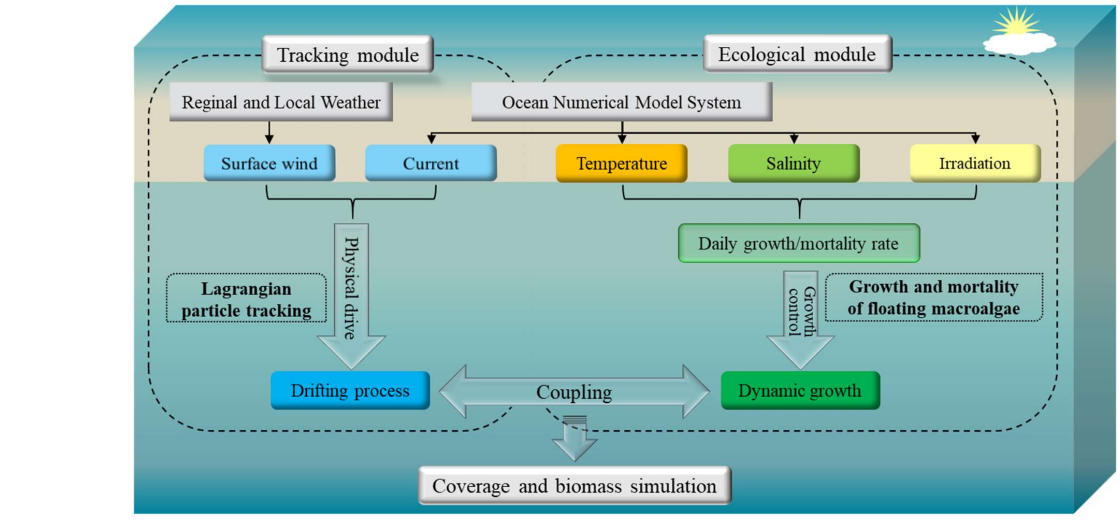

Figure 1. Framework of the physical–ecological coupled model FMGDM v1.0.

2.2 Lagrangian particle tracking module

Based on the hydrodynamic model, the Lagrangian particle tracking module was established. The current velocity $\vec{v}$ is obtained by spatial and temporal interpolation. Horizontal and vertical interpolations were carried out via linear interpolation, which was also used in the temporal scale. Surface wind contributes to the movement of macroalgae floating on the sea surface. Based on the size of macroalgae and the floating depth on the sea, surface wind accounted for 0–2 % of wind speed on the drifting of floating macroalgae. Additionally, the wind-induced Stokes drift also accounted for approximately 1.5 % of wind on the sea surface. Therefore, a total of 1.5–3.5 % (κ) of the 10-m-height wind velocity $\overrightarrow{V_w}$ was considered to determine the additional drifting velocity $\vec{V}$ of floating macroalgae. Assuming that κ is a fixed value, it does not change with the size of macroalgae in different life stages. The drifting velocity of floating macroalgae patches are determined using Eq. 1. Additionally, the drift speed is reduced when small patches of macroalgae aggregate as the spatial density ρ (unit: tons/km^2) increases. This effect was regarded as the assemble-induced slow-moving influence, κ_d, set based on Eq. 2.

$$\vec{V} = \vec{v} + \overrightarrow{V_w} \cdot \kappa \cdot \kappa_d \tag{1}$$

$$\kappa_d = \max\left(1 - \frac{\rho}{75}, 0.1\right) \tag{2}$$

To ensure the accuracy of particle trajectory, Eq. 3 is integrated by the fourth-order Runge-Kutta algorithm, and the time step of calculation Δt is 60s.

$$X_{t+\Delta t} = X_t + \int_t^{t+\Delta t} \vec{V}(x_t, t)dt \tag{3}$$

The random diffusion of the particles $\Delta\overrightarrow{x_r}$ is also considered in simulation as Eq. 4. The coefficient of random diffusion, K_r, was set to 200 m^2/s, and the time step Δt_{rd} for random diffusion was set to 6 s according to Visser's criterion. The unit vector $\vec{a}$ takes a random direction angle, and the random number R, fits normal distribution, takes a value between 0 and 1.0.

$$\Delta\overrightarrow{x_r}(t) = \int_t^{t+\Delta t} \vec{a} \cdot R\sqrt{2K_r t}dt \tag{4}$$

Therefore, the final position of Lagrangian particle tracking during one time step Δt can be expressed as:

$$X_{t+\Delta t} = X_t + \int_t^{t+\Delta t} \vec{V}(x_t, t)dt + \Delta\overrightarrow{x_r}(t) \tag{5}$$

https://doi.org/10.5194/gmd-2021-20
Preprint. Discussion started: 29 March 2021

Geoscientific Model Development Discussions

2.3 Ecological module

The growth and mortality of macroalgae are controlled by external environmental factors. Surface temperature θ, salinity S and irradiation intensity R of surface seawater were used to describe the physiological processes of macroalgae in our model. Daily growth/extinction rate δ (% day^{-1}) with θ, S, and R was determined using laboratory research results and revised according to the actual situation.

$$\delta_t = \delta(\theta_t, R_t, S_t, t) \tag{6}$$

The module reflects the process of growth and extinction of macroalgae by the replication and extinction of particles. One initial particle represented a patch with fixed biomass (m_0) of floating macroalgae and the value could be adjusted according to needs. It was randomly released within a 2-km radius of the original location when the represented biomass of the particle exceeded $2m_0$, and the biomass of the two particles returned to the initial value m_0. Both particles then underwent drifting and growth/extinction processes independently (Fig. 2a). Additionally, when both two nearby particles had biomass of below $0.5m_0$, they were combined to form one particle with a biomass of m_0, representing the extinction process (Fig. 2b). The calculation of dynamic change of single-particle biomass is expressed as:

$$m_{t+\Delta t} = m_t(1 + \delta_t \Delta t) \tag{7}$$

The total biomass of floating macroalgae throughout the domain can be determined by summing up the biomass of all active particles.

$$M_t = \sum_{n=1}^{N_t} m_{t,n} \tag{8}$$

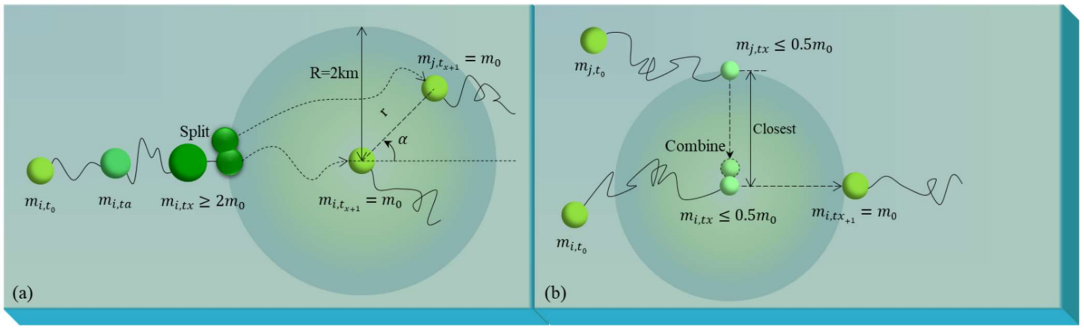

Figure 2. Diagram of the replication (a) and extinction (b) process of simulated macroalgae represented by particles.

2.4 Study area

Since their first bloom in YS in 2007, green tides have become a recurrent phenomenon over the past 13 years (Keesing et al., 2011; Xiao et al., 2020). The major macroalgal species involved in the green tide has been identified as *Ulva prolifera* (Ding and Luan, 2009; Duan et al., 2011). In contrast with some macroalgae that only bloom in certain areas such as coastal lagoons and estuaries, green tides, which account for most trans-regional macroalgal blooms worldwide (Liu et al., 2013), is much more complicated, both in spatial and temporal variations. The *U. prolifera* green tides in YS primarily originate from the coast of Jiangsu Province, primarily the coast of Yancheng and Nantong, and can drift northward to the southern shore of Shandong Peninsula and the coastal region of the Korean Peninsula (Liu et al., 2013; Son et al., 2012) (Fig. 3). Many loosely floating propagules of *U. prolifera* were provided from mid-Apr to mid-May every year (approximately 4000–6000 tons), which could float and grow in YS (Fan et al., 2015).

https://doi.org/10.5194/gmd-2021-20
Preprint. Discussion started: 29 March 2021

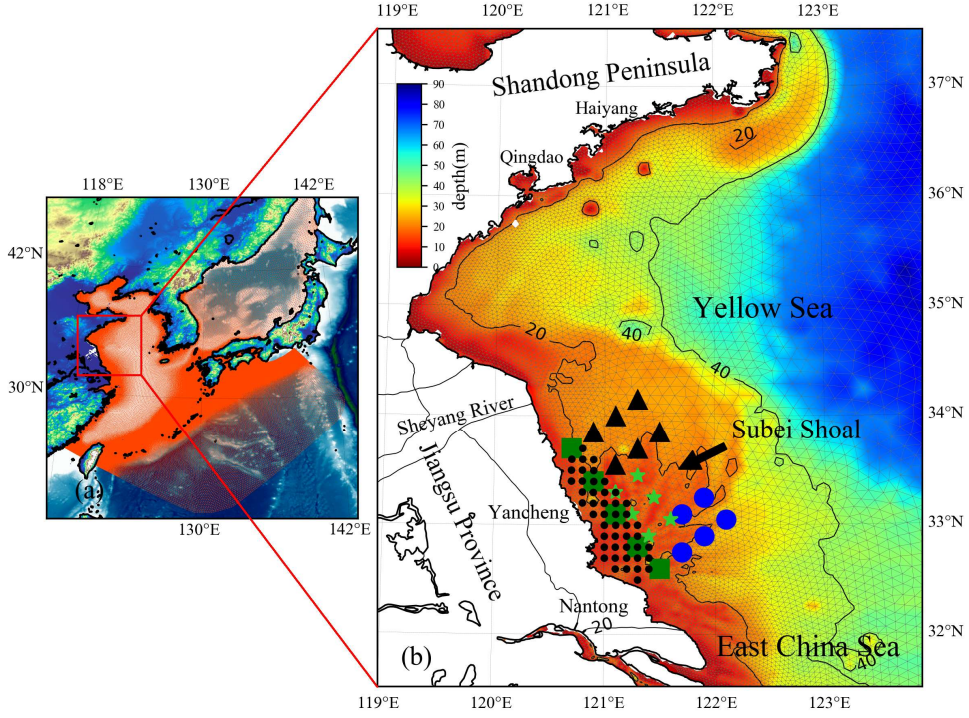

Figure 3. (a) Location of YS, China. The red mesh indicates the high-resolution triangle grids of ECS-FVCOM. (b) The enlarged view of the area and bathymetry bounded by the solid red line rectangle in panel (a). The green squares, blue bullets, and triangle indicate the positions of particles released on the coast, southern and northern regions of the Subei Shoal, respectively. The lime green stars indicate that the initial position of the tracking simulation only considers the action of ocean flows. Black dots indicate the position of the 47 initial particles released for simulation in 2014 and 2015.

2.5 Data sources

2.5.1 Surface wind

The wind data at 10 m above sea level derived from the surface wind dataset from the European Centre for Medium-Range Weather Forecasts (ECMWF) are available at: https://www.ecmwf.int/en/forecasts/datasets/. The wind is interpolated to the triangular grids, covering YS, East China Sea, Bohai Sea, and Japan Sea, in spatial and time scale. The interpolated wind data was used as surface forcing for ECS-FVCOM, with the spatial resolution of 0.125° and temporal resolution of 1 h.

2.5.2 Satellite data

The distribution area and density of green tides can be estimated from satellite data (Hu et al., 2019; Qi et al., 2016). In this study, the spatial distribution and growth density of green tides of the simulation were validated using satellite data. The satellite data of green tides in YS in 2014 and 2015 are available from https://terra.nasa.gov/about/terra-instruments/modis, the Moderate Resolution Imaging Spectroradiometer with Terra sensor (MODIS-TERRA). In addition, the biomass quantified based on the satellite data from Hu et al. (2019) was used to verify the simulated *Ulva prolifera* biomass. Remote sensing techniques exhibit difficulty in detecting small patches of floating macroalgae and may easily fail to capture the early status of green tides (Garcia et al., 2013). Only a few remote sensing observations that were not blocked by clouds can be used for result verification.

https://doi.org/10.5194/gmd-2021-20
Preprint. Discussion started: 29 March 2021

Geoscientific Model Development Discussions

The remote-sensing dataset from https://www.ghrsst.org/, Group for High-Resolution Sea Surface Temperature (GHRSST), is used for data assimilation of sea surface temperature in the model system. The GHRSST dataset is daily based, with a spatial resolution of 0.01 degrees.

2.6 Hydrodynamic model

An unstructured-grid, Finite-Volume Community Ocean Model (FVCOM) adapts to the second-order accurate discrete flux algorithm in the integral form to solve the governing equations on an unstructured triangular grid, which provides excellent mass and momentum conservation during the calculation (Chen et al., 2006; Chen et al., 2007; Chen et al., 2003; Ge et al., 2013). To better identify the ocean circulation along the shelf break and deep ocean, semi-implicit discretization, which could avoid the adjustment between two-dimensional external mode and three-dimensional internal mode, was applied. With this configuration, the ocean circulation, as well as the astronomical tide around the East China Sea, YS and adjacent region, could be reasonably determined (Chen et al., 2008; Ge et al., 2013). An integrated high-resolution numerical model system for the East China Sea (ECS-FVCOM) based on FVCOM v4.3 (http://fvcom.smast.umassd.edu/fvcom/) was established and comprehensively validated using observational data (Chen et al., 2008; Ge et al., 2013). The high-resolution triangle grids of ECS-FVCOM domain covers YS, East China Sea, Bohai Sea, and Japan Sea, which have horizontal resolutions varying from 0.5–1.5 km in the estuary and coastal region, approximately 3 km in the path of the Kuroshio, and 10–15 km along the lateral boundary in the north Pacific region (Fig. 3a). A total of 40 generalized sigma layers are considered in the vertical, including five uniform layers with a thickness of 2 m specified in the sea surface and bottom to better resolve surface heating and wind mixing, and bottom boundary layer (Chen et al., 2008). The ocean bathymetry was retrieved and interpolated from ETOPO1 (https://ngdc.noaa.gov/mgg/global/global.html). The initial temperature/salinity field and the volume transports along the open boundary of ECS-FVCOM were interpolated and retrieved, from HYCOM+NCODA Global 1/12° Analysis data (GLBA0.08), and eight major tide harmonic constituents (M2, S2, K2, N2, K1, O1, P1, and Q1), which are obtained from TPXO 7.2 Global Tidal Solution (Egbert and Erofeeva, 2002), were used along the open boundary (Ge et al., 2013). The freshwater discharge of the Yangtze River and Qiantang River (source: http://www.cjh.com.cn/) was added to the upstream river boundary. Surface wind and radiations from ECMWF were used in ECS-FVCOM as surface forces. In addition, the Group for High-Resolution Sea Surface Temperature (GHRSST) dataset was applied to better determine the sea surface temperature using the model data assimilation. The simulation time was set from March 29 to September 1, thus covering early spring to late summer. The water velocity, temperature, salinity from ECS-FVCOM were fed into the FMGDM as input variables.

2.7 Model settings

The model was parameterized according to the physiological characteristics of the floating *U. prolifera*. Furthermore, 2 % of wind speed was accounted for by the drifting of floating *U. prolifera*, and 1.5 % of wind was accounted for by the wind-induced Stokes drift. Therefore, the coefficient κ was set to 3.5 % (Bao et al., 2015). Based on many physiological research studies on *U. prolifera*, the optimal range of temperatures, irradiance, and salinity can be determined (Table 1). Owing to the protection of the dense branch, floating *U. prolifera* are more tolerant of high irradiance in fields than in the laboratory (Xiao et al., 2016). In the optimal environment range, the daily growth rate of floating *U. prolifera* can reach 10.6–16.7 % (Xiao et al., 2016). Therefore, the relative growth rate of the *U. prolifera* growth module was set refer to the results of physiological research and actual growth in fields. (Table 2).

Table 1. Optimal range of temperatures, irradiance and salinity during *U. prolifera* growth

Environmental factors	Lower limit	Suitable	Upper limit	Reference
Temperature (°C)	10	14 – 27	30	Xiao et al. (2016)
Irradiance (μmol photons m^{-2} s^{-1})	–	200 – 2400	2400	Cui et al. (2015) Xiao et al. (2016)
Salinity (psu)	8	26 – 32	–	Xiao et al. (2016)

https://doi.org/10.5194/gmd-2021-20
Preprint. Discussion started: 29 March 2021

Geoscientific Model Development Discussions

Table 2. Relative growth rate setting of *U. prolifera* growth model at various temperatures, irradiance and salinity.

Environmental factors			Relative growth rate (% d^{-1})
Salinity (psu)	Temperature (°C)	Irradiance (μmol photons m^{-2} s^{-1})	
26 – 32	< 10	⩾ 0	0
	10 – 14	0 – 200	2
		200 – 3200	7
		⩾ 3200	2
	14 – 25	0 – 200	5
		200 – 3200	22
		⩾ 3200	5
	25 – 27	0 – 200	0
		200 – 3200	2
		⩾ 3200	-2
	27 – 29	⩾ 0	-12
	⩾ 29	⩾ 0	-90

To determine the drift trajectory of *U. prolifera* in the natural state and understand the contribution of these physical factors, two particle-tracking experiments were designed. Three group particles were released on May 1, 2014 in the coastal, southern, and northern regions of the Subei Shoal respectively (Fig. 3b). The roles of ocean circulation and surface wind were considered in this tracking experiment, and the simulation lasted 120 d. Meanwhile, the other tracking experiment was configured with mostly the same settings, but the effect of surface wind on floating particles was disregarded. In the second experiment, initial particles were also released on May 1, 2014 but only around the Subei Shoal (Fig. 3b).

Most importantly, two realistic dynamic growth simulations were conducted. To verify the general applicability of the model, the growth and drift processes of *U. prolifera* in YS in 2014 and 2015 were simulated, respectively, with identical model configurations. In the two simulations, a total of 47 particles were initially released into the Subei coast on May 1, 2014 and 2015, uniformly distributed in space (Fig. 3b). One initial particle represented a patch of 100 tons of floating *U. prolifera*. This suggested that the initial biomass of *U. prolifera* was approximately 4,700 tons. This approximate coverage and biomass of the initial *U. prolifera* was determined according to the survey by Liu et al. (2013) and Xu et al. (2014). The simulation continued for 120 d from spring to the end of the summer. In this study, instantaneous environmental factors, including temperature, salinity, currents, and solar radiation intensity, were determined according to corresponding positions where the particles were floated from the physical ECS-FVCOM model.

3 Results

3.1 Variations of environmental factors

3.1.1 Surface wind

The wind vectors at 10 m height near Subei coast and Qingdao coast, which were retrieved from ECMWF was showed in Figure 4. From May to July 2014, southerly and southeasterly winds prevailed in the coast of Subei and Qingdao, and the mean wind speed reached 5 m/s. However, the southerly wind was stronger throughout May in Spring. In June, southeast winds blew in the Subei coast significantly and the Qingdao coast was still dominated by southerly wind, the wind speed was slightly lower than that in May. In August, the northeast wind was strengthened, especially from August 1–10.

https://doi.org/10.5194/gmd-2021-20
Preprint. Discussion started: 29 March 2021

Geoscientific Model Development Discussions

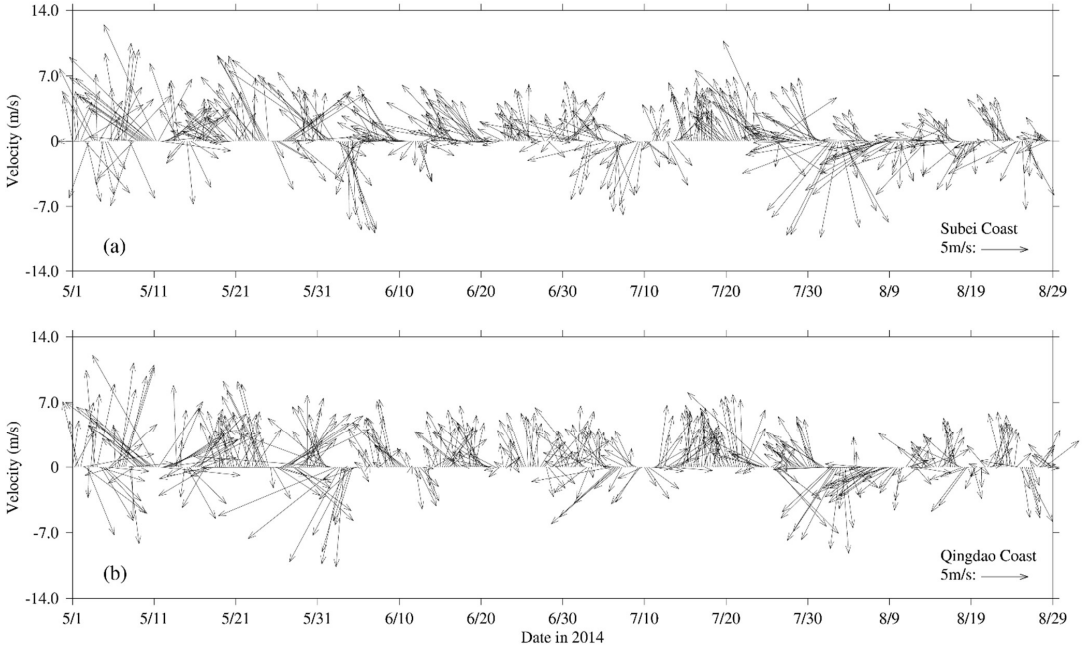

Figure. 4. Wind vectors at 10 m height near Subei coast (a) and Qingdao coast (b) at a time interval of 6 h from May to August 2014.

3.1.2 Ocean circulation

The time-averaged distributions of surface ocean circulation every 15-d period in 2014 and 2015 are shown in Figs. 5 and 6, respectively. Affected by the southerly and southeasterly winds (Fig. 4), the coastal surface seawater flowed northward and was transported to the east of South YS. This phenomenon was more pronounced in May and late June and July (Fig. 5a, b, d, f), indicating the possibility of *U. prolifera* drifting from Subei Shoal toward the north. The same phenomenon was observed from May–June, and early August of 2015 (Fig. 6a–d, g). Most of the time, surface seawater from north YS was transported to South YS through the east of Rongcheng (RC). In early June and July and August 2014 (Fig. 5c, e, g, h), the surface seawater circulated counterclockwise in the middle region of South YS. Simultaneously, the weak currents on the south side of the Shandong Peninsula may have caused *U. prolifera* to stay in this region and gradually land on the shore. Similar ocean circulations appeared in July and late August of 2015 (Fig. 6e, f, h), and weak northward currents were observed on Subei Shoal.

3.1.3 Temperature

Figures 5 and 6 also included the distribution of surface seawater temperature in 2014 and 2015 respectively, with every 15-d time averaging. The average temperature of South YS reached 13 °C in May (Fig. 5a, b) and increased continuously in June (Fig. 5c, d). Surface seawater temperature along Jiangsu Coast and the East China Sea was generally 1–2 °C higher than that in other areas of South YS. However, most of South YS reached a high-temperature state, with over 25 °C, by July 2014 (Fig. 5e, f). From mid-July to end-August, the surface temperature in Jiangsu Coast and parts of Shandong Peninsula Coast remained above 27 °C (Fig. 5f–h). The offshore sites of Qingdao and Subei were selected to determine the time series process for the physical factors (Fig. 5i–j and Fig. 6i–j). The surface temperatures of two stations, the northern Jiangsu Coast and Qingdao coast, were increased until they reached their peaks at the end of July with over 27 °C and remained until the end of August.

https://doi.org/10.5194/gmd-2021-20
Preprint. Discussion started: 29 March 2021

The distribution and tendency of South YS seawater temperature in 2015 were similar to those in 2014 (Fig. 6). However, compared with those in 2014, they had more extensive high-temperature coverage for South YS in August 2015 (Fig. 6g–h). The surface temperature of most YS regions exceeded 27 °C, part of the Jiangsu Coast even reached 29 °C. In addition, the surface temperatures of the two stations reached 25 °C in 2015, approximately one week later than they did in 2014 (Fig. 6i–j).

3.1.4 Irradiation and salinity

Solar irradiation intensity is significantly different in the day and night. Therefore, only the irradiation intensity at 12:00 am was analyzed in Fig. 5i–j and Fig. 6i–j. Affected by the thickness of clouds, irradiation intensity at noon fluctuated drastically within 3200 $\mu mol \cdot m^{-1} \cdot s^{-1}$. Compared with May and June, the irradiation intensity in July and August of 2014 and 2015 decreased slightly.

Because the Qingdao is far from the Changjiang Estuary (CJE) where the freshwater discharge enters the shelf region, the seawater salinity at Qingdao exhibited weak variations, which were maintained within the range of 31.5–32.0 PSU (Fig. 5i and Fig. 6i). However, the seawater salinity around Subei coastal region was significantly affected by the influence of the fresh water that flowed into Subei sea in summer. It dropped from approximately 32.0 PSU to approximately 30.5 PSU from May to the end of August 2014 (Fig. 5j) and to 30.0 PSU in July and August of 2015 (Fig. 6j). The surface salinity of South YS fluctuated between 29 PSU and 33 PSU during the period of the green tide bloom, which was suitable for *U. prolifera* growth (Xiao et al., 2016).

https://doi.org/10.5194/gmd-2021-20
Preprint. Discussion started: 29 March 2021

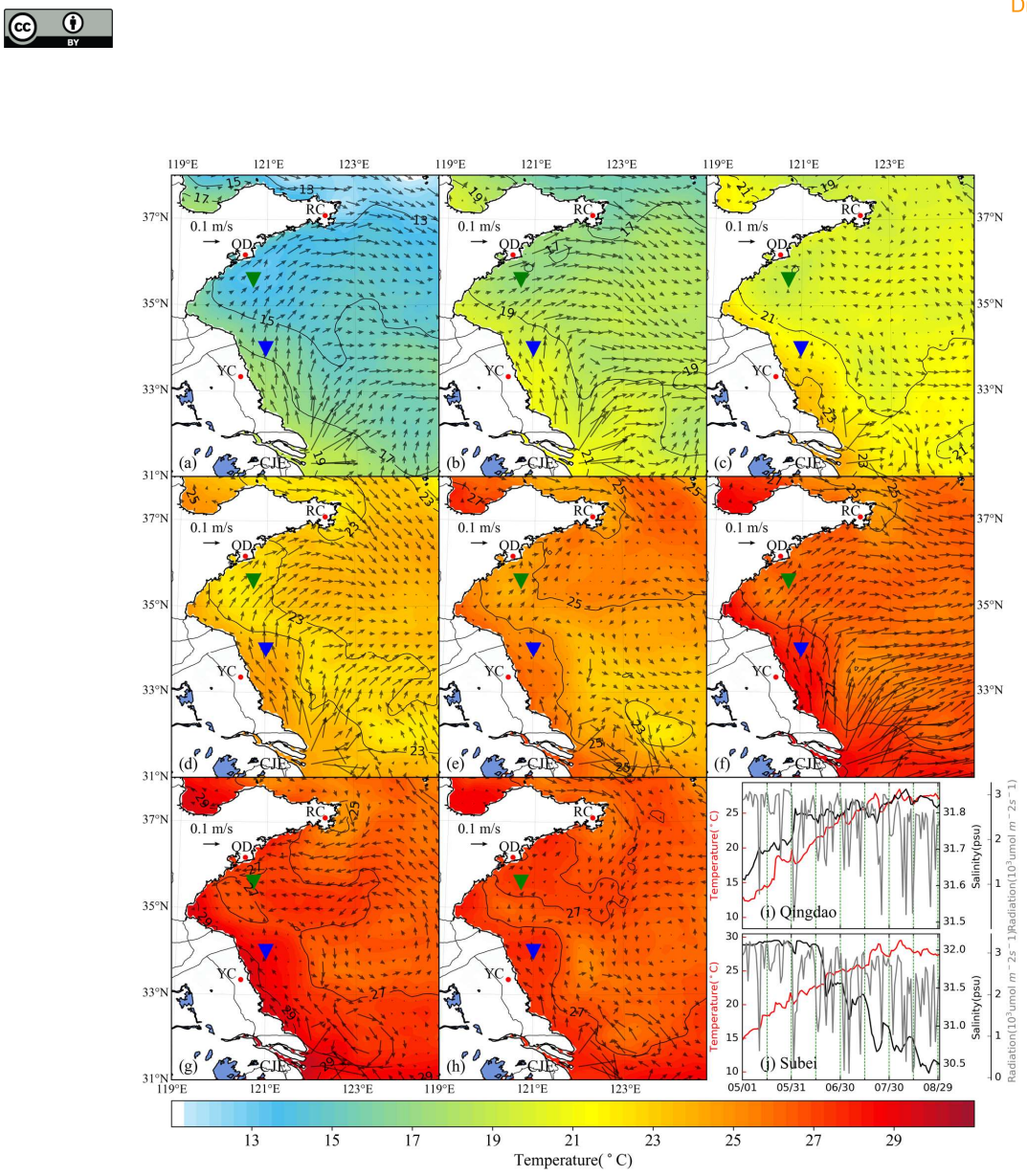

Figure. 5. Time-averaged distribution of surface current and temperature of every 15-d duration in 2014: (a) 1–15 May, (b) 16–30 May, (c) 31 May–14 June, (d) 15–29 June, (e) 30 June–14 July, (f) 15–29 July, (g) 30 July–13 August, (h) 14–29 August. The green and blue inverted triangle indicate the position of selected Qingdao (QD) coast and Subei offshore sites, respectively. Time series of surface temperature, salinity, and irradiation in Qingdao (i) and Subei (i).

https://doi.org/10.5194/gmd-2021-20
Preprint. Discussion started: 29 March 2021

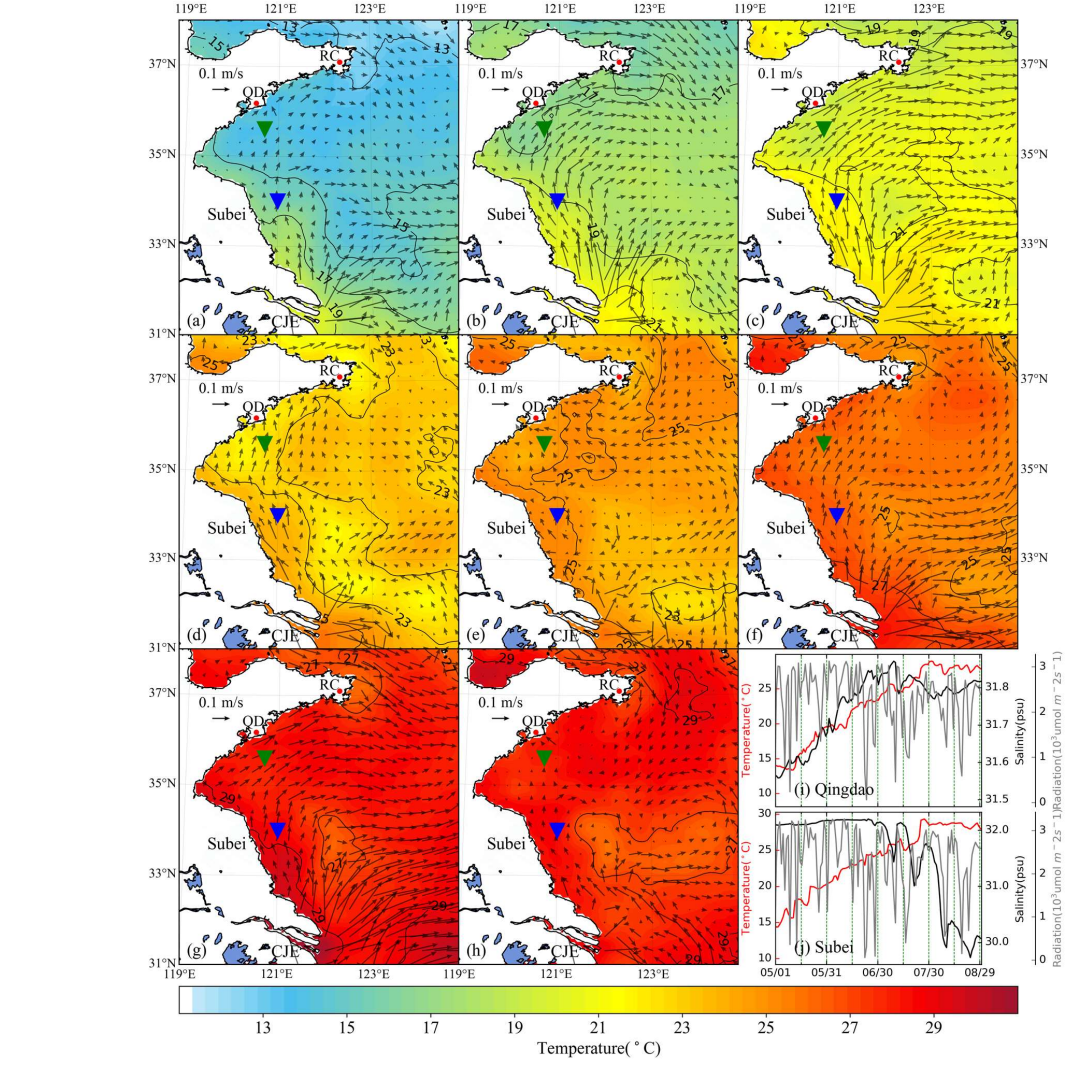

Figure. 6. Time-averaged distribution of surface current and temperature of every 15-d duration in 2015: (a) 1–15 May, (b) 16–30 May, (c) 31 May–14 June, (d) 15–29 June, (e) 30 June–14 July, (f) 15–29 July, (g) 30 July–13 August, (h) 14–29 August. The green and blue inverted triangles indicate the position of selected Qingdao (QD) coast and Subei offshore sites, respectively. Time series of surface temperature, salinity, and irradiation in Qingdao (i) and Subei (i).

3.2 Effects of physical factors

3.2.1 Wind

The drift trajectory of the floating *U. prolifera* was simulated from May 1 to August 29. Three groups of initial particles were released in three regions of the Subei Shoal (Fig. 3b). In this experiment, the roles of both wind and ocean circulation were considered. Results of the experiment showed that the particles significantly drifted northward in May and then turned northeastward under the influence of south and southeast wind (Fig. 7a–c). The particles released along the coast of Subei could drift to the south side of the Shandong Peninsula in mid-June and float on the north of YS throughout August (Fig. 7a). Similar to Fig. 5a, the particles released from the north side of Subei Shoal were transported northeast, and most of the particles

https://doi.org/10.5194/gmd-2021-20
Preprint. Discussion started: 29 March 2021

cannot drift out of north YS (Fig. 7b). The particles released from the south side of Subei Shoal demonstrated a stronger tendency to drift eastward, which could drift to the west coast of the Korean Peninsula (Fig. 7c). These drift patterns were all a result of the full effects of wind and circulation.

3.2.2 Ocean circulation

The other experiment was conducted with the exclusion of the wind effect, meaning that the particles are driven only by the ocean flows. Initially, six particles were released into Subei Shoal on May 1, 2014 (lime green stars in Fig. 3b). After one and a half months of simulation, simulated particles were still floating within Jiangsu Coast and then turned northeastward under the role of the circulation to the central part of YS in July and August (Fig. 7d). Simulation results suggested that floating green tides cannot be transported out of Jiangsu Coast within a short period, but these particles still tended to move northward via wind-driven current. The drift trajectory near the initial position of particle release showed obvious spiral oscillations caused by rotary tidal current. When the particles moved to the shore or north Subei Shoal, the trajectories showed small-scale north–south oscillation that may be attributable to alternating tidal current. However, the net transport made by periodical alternating tide current was quite limited, resulting in slow northward movement of surface particles. These two experiments with/without wind suggest the offshore extension of *U. prolifera* from the Subei Shoal to the central YS was primarily caused by the wind-induced drift. Additionally, the ocean circulation primarily caused the northward drifting of *U. prolifera*. Therefore, under the jointed effects of circulation and wind, the *U. prolifera* could detach quickly from *Porphyra* aquaculture raft from Subei Shoal.

https://doi.org/10.5194/gmd-2021-20
Preprint. Discussion started: 29 March 2021

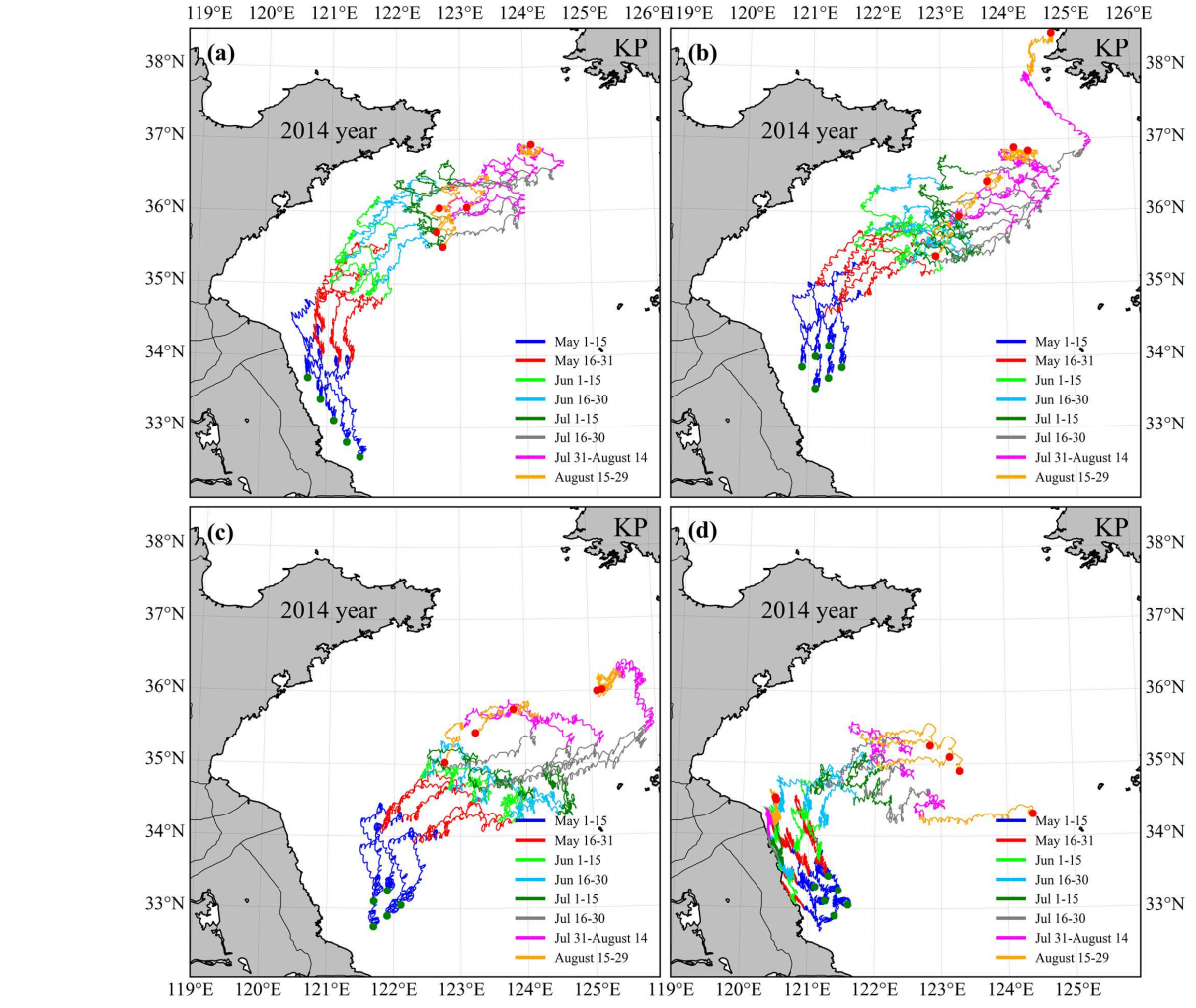

Figure 7. Drift trajectories from wind-circulation (a–c) and circulation-only (d) experiments. Green bullets indicate the initial positions of particles. Drift trajectory simulation for particles released along coast (a), on northern (b), and southern (c) of the Subei Shoal. Different colors are used to denote 15-d sub-periods from May 1 to August 29, 2014.

3.3 Simulation of dynamic growth model

3.3.1 Biomass of green tide

As there was no direct way of quantifying the floating *U. prolifera* biomass of green tides throughout the YS (Wang et al., 2018), the estimated biomass data of *U. prolifera* retrieved from remote sensing observations (Hu et al., 2019) was adopted to validate the simulated biomass (Fig. 8). Satellite observations of a small amount of floating *U. prolifera* in YS were made in mid-May. Until mid-June, the estimated biomass of *U. prolifera* rose rapidly and peaked on June 18, 2014 (Fig. 8a), and June 21, 2015 (Fig. 8b), separately, with maximum values of 0.92 million tons and 1.98 million tons, respectively. After peaking, the biomass declined rapidly, and *U. prolifera* almost died off at the end of July. The observed biomass trends in 2014 and 2015 were similar, showing an inverted V shape.

https://doi.org/10.5194/gmd-2021-20
Preprint. Discussion started: 29 March 2021

Geoscientific Model Development Discussions

After the initial particles were released, the green tide simulation began, with the coupling between physical drifting and biological growth. Compared with observation results, the biomass of simulation peaked after 12 d and 10 d, respectively, with a higher maximum value, 1.77 million tons on July 30, 2014 (Fig. 8a), and 2.31 million tons on June 1, 2015 (Fig. 8b). The growth trends were similar to the observations. Considering the highly random distributions, as well as the robust dynamic life history of *U. prolifera*, our simulation provided reasonable modeling results of biomass.

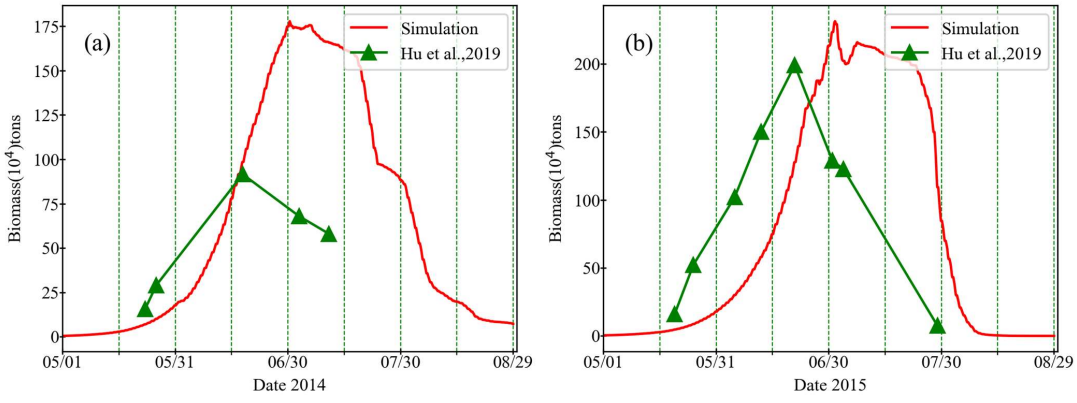

Figure 8. Comparison between simulated (red) and observed (green) biomass of green tide in 2014 (a) and 2015 (b). observed values were sourced from the study by Hu et al. (2019).

3.3.2 Spatiotemporal variation of *U. prolifera*

After being released into Subei Shoal, the initial particles drifted and diffused driven by ocean flows and wind. The simulation result of the green tide in 2014 is shown in Fig. 7. It showed a small amount of *U. prolifera* floating on Subei coast in mid-May (Fig. 9a). However, it was difficult to be observed using remote sensing technology in the early stage of green tide bloom. After approximately one month of simulation, the modeling biomass increased to approximately 300 thousand tons (Fig. 9i). Both the result of observation and simulation showed that *U. prolifera* were transported northward and floated between northern Jiangsu offshore and Shandong Peninsula (Fig. 9b). On June 15 (Fig. 9c), observation shows that green tides had landed on the southern coast of Shandong Peninsula including Rizhao (RZ) and Qingdao shore. Meanwhile, the floating simulation was also close to these two sites. Moreover, observation shows that green tides bloomed around the coast of Nantong (NT) and Yancheng (YC), suggesting the continuous release of additional *U. prolifera* from aquaculture raft between May and June, 2014. On June 30 (Fig. 9d), the result of both observation and simulation were consistent and showed that green tides had landed on the Shandong Peninsula on a large scale, and the farthest *U. prolifera* reached the Rushan (RS) coast. The entire coast and offshore were covered with a huge amount of floating *U. prolifera.* The biomass of simulation reached a peak of 1.77 million tons (Fig. 9i). On July 17 (Fig. 9e), the floating *U. prolifera* was still gathered and grew on the south coast of the Shandong Peninsula. In contrast with the simulation results, observation showed the reoccurrence of a large-scale green tide in Jiangsu Coast, which could not be simulated. It also suggested the continuous drifting of *U. prolifera* from the Subei region, which was not considered in the simulation. Subsequently, *U. prolifera* died out quickly, and its coverage decreased significantly. The results of both observation and simulation show that floating drifted eastward but still covered the south coast of the Shandong Peninsula at the end of July (Fig. 9f). After half a month, floating *U. prolifera* had died out (Fig. 9g). Observation shows that only the southern coast of Qingdao and Subei Shoal had a few patches of *U. prolifera* on August 14. The floating patch on Qingdao coast could be simulated, and some *U. prolifera* on the southern coast of Rongcheng survived. At the end of August, green tides in YS almost vanished, which could not be detected by the satellite remote sensing (Fig. 9h). The biomass of the simulation was less than 10 thousand tons.

https://doi.org/10.5194/gmd-2021-20
Preprint. Discussion started: 29 March 2021

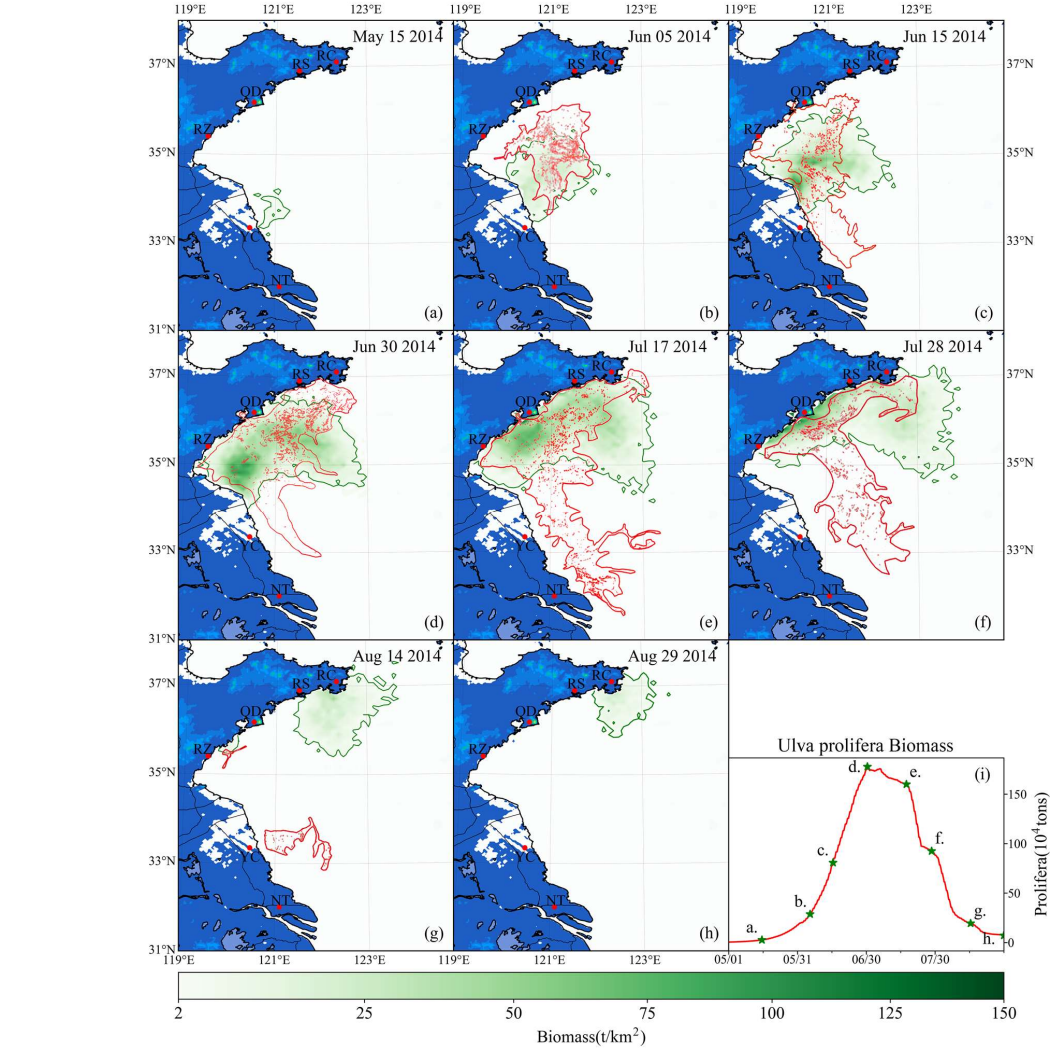

Figure 9. Comparison between simulation and remote sensing observation of green tides from May to August 2014 (a–h). The green image indicates the simulated biomass density of green tides (color image, unit: tons/km^2), and the red image indicates the satellite-derived spatial coverage of *U. prolifera* from MODIS-TERRA. Panel (i) is the time series of simulated biomass of green tides in 2014, and the green pentagram indicates the biomass of the corresponding date in the panel (a–h).

To verify the reliability of the coupled model system, the green tides that bloomed in 2015 were also simulated and compared with the observations made. The simulation shows that a small amount of *U. prolifera* was floated near the coast of Jiangsu in mid-May (Fig. 10a). On May 30, the coverage of floating *U. prolifera* increased, while the northernmost green tide patches reached 35°N (Fig. 10b). Observation shows that, on June 23, green tides entered the Shandong Peninsula with large-scale coverage, distributed in most of the seas from Subei to Shandong Peninsula and bloomed strongly offshore of Qingdao to RS (Fig. 10c). The coverage of simulation results was similar to the observation, but the high-density area was close to Jiangsu. In addition, observation showed scattered patches of *U. prolifera* floating in the far sea of the South YS. On July 2, both observation and simulation showed that green tide still gathered along the south coast of the Shandong Peninsula, and the northernmost of the distribution range reached RC (Fig. 10d). Simulated biomass peaked at a maximum value of more than 2

https://doi.org/10.5194/gmd-2021-20
Preprint. Discussion started: 29 March 2021

Geoscientific Model Development Discussions

million (Fig. 10i). On July 16 (Fig. 10e), satellite observation showed that the coverage of green tide reduced greatly, and the distribution range was shrunk toward the west of 121°E. However, compared to the situation on July 2, the distribution of simulation changed only slightly, and the total biomass fluctuated within proximity to the peak (Fig. 10i). The simulated green tides then vanished rapidly. Floating *U. prolifera* gathered primarily along the coast of RZ and Qingdao (Fig. 10f). Biomass of simulation dropped to about one million tons at the end of July (Fig. 10i). On August 5, observations showed small patches of floating green tide in the middle of South YS (Fig. 10g). In simulation results, a small amount of green tide remained along the coast. On August 20 (Fig. 10h), the green tide of YS completely disappeared from satellite observation and numerical simulation.

The entire process of green tide growth and drift in 2014 and 2015 could be adequately determined by this dynamic growth and drift model. The differences between the simulated and observed results are discussed in Section 4.

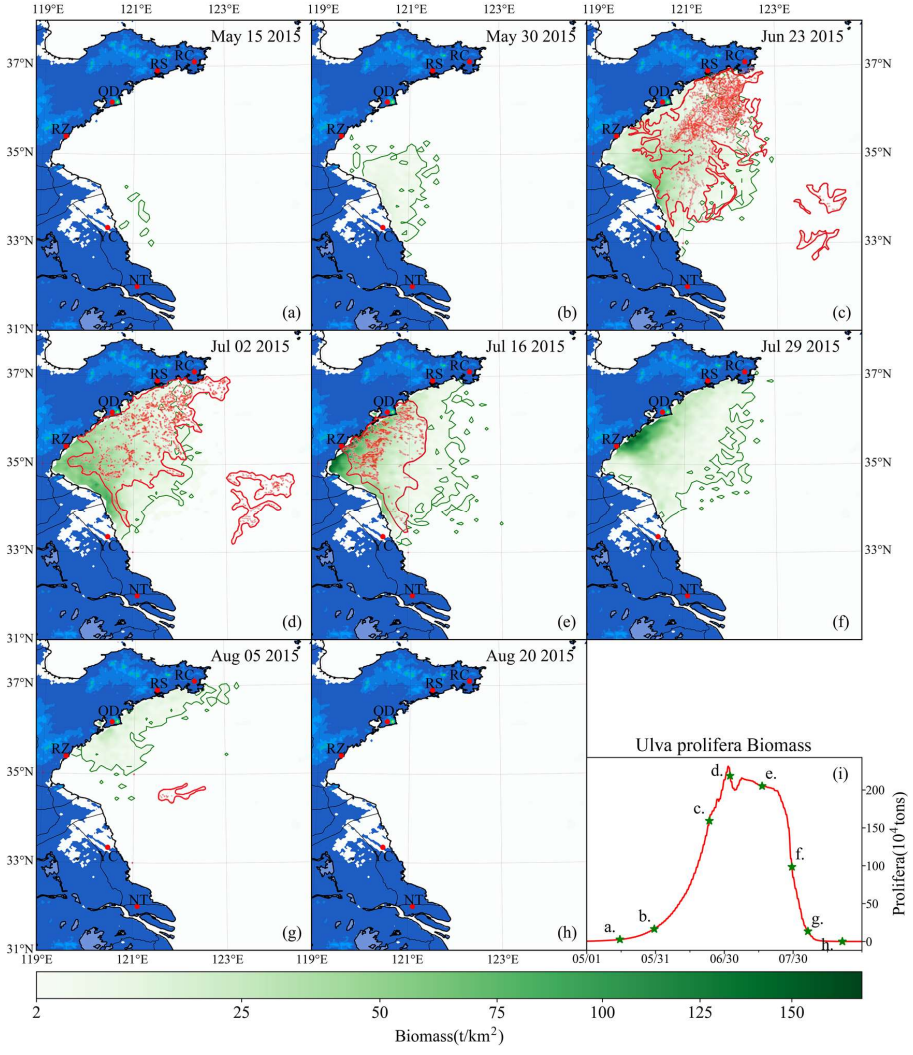

Figure 10. Comparison between simulation and remote sensing observation of green tide from May to August 2015 (a–h). The green image indicates the simulated biomass density of green tide (color image, unit: tons/km^2); the red image indicates the satellite-derived spatial coverage of *U. prolifera* from MODIS-TERRA. Panel (i) is a time series of simulated biomass of green tide in 2014, the green pentagram indicates the biomass of the corresponding date in panel (a–h).

https://doi.org/10.5194/gmd-2021-20
Preprint. Discussion started: 29 March 2021

4 Discussion

4.1 Uncertainties of physical, biological and anthropic processes

The observation of the entire bloom process is technically complex in the study of massive floating macroalgal blooms. Following the establishment of floating macroalgae growth and drift model in this study, and supplemented by remote sensing observations, the entire process of growth and drift under floating could be re-produced and bloom development predicted. However, there are many uncertainties throughout the blooming process from early spring to late summer, which could significantly limit the precision of long-term prediction.

In the realistic numerical simulations of green tides from 2014 to 2015, the initial biomass of *U. prolifera* had the same configuration of 4700 tons on May 1 from the estimation in previous studies ((Liu et al., 2013; Xu et al., 2014). The initial distribution was also uniform. However, high uncertainties regarding the biomass and distribution were observed. The initial biomass of *U. prolifera* was determined primarily by the scale of local *Porphyra* aquaculture around the Subei coastal region and the timing of harvest activities. The precise estimation of initial biomass and timing requires extensive monitoring for these activities, as well as robust and timely satellite assessment of satellite remote sensing.

From the satellite observations in June and July 2014, we observed stable patches of *U. prolifera* off the Subei Shoal (Fig. 9c–e). This indicated the continuous drift of *U. prolifera* from the local *Porphyra* aquaculture activities, resulting in stable bloom off the Subei Shoal and northward drift. Therefore, this factor should be considered during long-term simulation; otherwise, it could lead to extensive bias of *U. prolifera* distribution and biomass.

During the bloom of green tides, large-scale salvage operations were implemented to reduce the biomass of floating *U. prolifera* in Jiangsu and Shandong coastal waters (Liu et al., 2013; Wang et al., 2018). This could significantly change the local biomass. The biomass of salvage operations reaches 1.5–2.0 × 10^6 tons every spring and summer along the Shandong coastal region (Ye et al., 2011; Zhou et al., 2015), which could be the reason for the underestimation of biomass from June 2–16, 2015 (Fig. 10d–e). The salvage operations cause significant uncertainty for numerical prediction, particularly along the coast where the operations are primarily conducted.

The propagules are distributed near the floating Ulva with a high density and move together with ocean flows (Li et al., 2017). The modified clay (MC) at a proper dose can flocculate with microscopic propagules and effectively remove microscopic propagules from the water column (Li et al., 2020b). The physiological processes of *Ulva* cells could be disrupted by MC (Zhu et al., 2018). This method was frequently used to mitigate blooms in local areas (Li et al., 2017). The intervention of human activities on the blooming process was not considered in the model. When the observed biomass peaked, the biomass in the simulation maintained an increasing trend. The maximum simulated biomass was larger than the maximum estimated biomass, and the duration of the bloom was longer than that of the actual condition. Large-scale salvage and elimination activities play important roles in reducing the scale and intensity of the green tide bloom.

4.2 Short-term variations and quick response

To reduce the errors of long-term simulation, caused by the complex origin of initial floating macroalgae and the uncertainty of growth and drift, the time of each simulation was shortened by dividing the entire long-term simulation into multiple short-term simulations and renewed the location and biomass in every short-term modeling by initialization of floating estimated by remote sensing observation.

Two consecutive simulations were carried out during the heyday of YS green tides. One was configured for simulations from June 15–23, 2014, and the other from June 23–30, 2014. According to the distribution from remote sensing observation and estimated biomass from Hu et al. (2019), the initial biomass and distribution of *U. prolifera* on June 15, 2014 was determined as shown in Fig. 11a and June 23, 2014 in Fig. 11d. The initial biomass was approximately 0.7 million on June 15 and approximately 0.96 million on June 23.

https://doi.org/10.5194/gmd-2021-20
Preprint. Discussion started: 29 March 2021

Geoscientific Model Development Discussions

The time interval between two consecutive clear satellite observations of green tides was generally large. Two intermediate results between the gap of satellite observation were shown in Figs. 11b and 11e. After nearly one-week of simulation, the coupled model system made precise simulation, compared with remote sensing (Fig. 11c, f), and the biomass was consistent with that estimated via satellite remote sensing (Fig. 11g). Moreover, spatial distribution was well predicted. Compared with long-term simulation, the variation of green tide distribution and biomass could be determined more accurately by the results of the short-term simulation. The accuracy of short-term simulations is reliable, and the short-term prediction of floating macroalgal blooms can be achieved by combining the numerical model with the satellite observation.

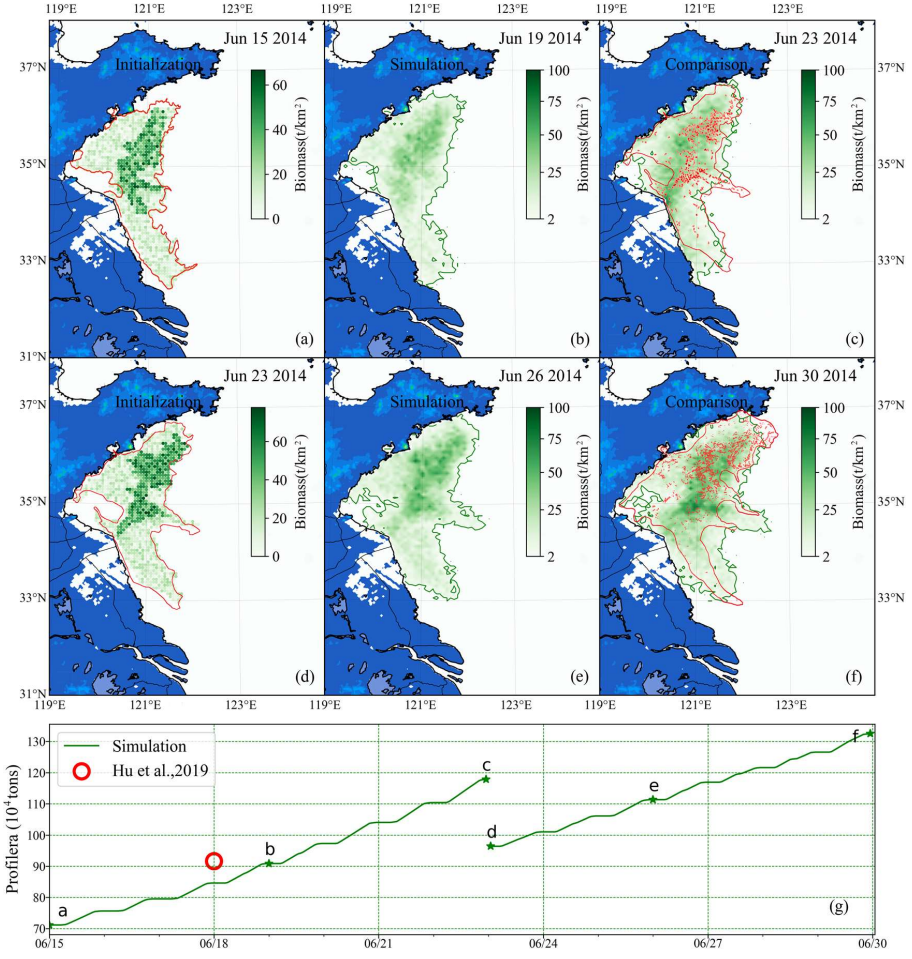

Figure 11. Comparison of short-term simulation and satellite observation of green tides in 2014: position and distribution of green tide density released initially: 15 June (a) and 23 June (d) based on the satellite date and estimated biomass. Panels (b) and (e) are the modeling results of 19 June and 26 June, respectively. Panels (c) and (f) are the comparison between simulation and satellite observation on June 23 and June 30, respectively. The green image indicates the simulated result and the red one indicates satellite observation. Panel (g) is the comparison of two consecutive simulated biomass (green line) and estimation biomass of satellite data (red circle). The green pentagrams indicate the biomass of the corresponding date in panels (a–f).

https://doi.org/10.5194/gmd-2021-20
Preprint. Discussion started: 29 March 2021

4.3 Roles of initial biomass and nutrient limitation

The existence of diverse origins and continuous input of floating propagules greatly challenge the precise prediction and effective control of massive floating macroalgal blooms. In addition to the large provision from *Porphyra* aquaculture rafts in Subei Shoal, the somatic cells, indicated by a laboratory study, could overwinter and restore growth on the annual spring bloom (Zhang et al., 2009), which is another significant source of *U. prolifera*. Additionally, four overwintering *Ulva* propagules that existed in sediments, including *U. prolifera*, may recover their growth when the temperature and irradiation are appropriate (Liu et al., 2012). Every April, before the occurrence of green tides, *Ulva* propagules are already widespread on the southern coast of YS (Yuanzi et al., 2014). The transport trajectory was strongly affected by the origin of *U. prolifera* (Fig. 5). Under the same environmental conditions, the scale of the bloom was determined primarily by the initial organisms. During the macroalgal bloom, the propagules supply from the coastal waters is continuously uncertain and difficult to determine through satellite observation or in-situ surveys. Therefore, as shown by satellite observations, there was still large-scale *U. prolifera* distribution around Subei Shoal in June and July 2014 (Fig. 9). However, as the continuous biomass entering into the ocean was not included in our simulation, this feature has not yet been determined.

In addition to the temperature, irradiation, and salinity, environmental factors that affect the growth of macroalgae, such as dissolved nutrients (Li et al., 2020a; Wang et al., 2019), were not considered in this model. Floating *U. prolifera* can efficiently absorb nutrients (Luo et al., 2012), and the concentration of nutrients in the sea would decrease sharply when *U. prolifera* blooms dramatically, which may hinder the rapid growth of *U. prolifera* (Wang et al., 2019). When the actual growth of green tide bloom reached its peak with millions of tons of biomass, dissolved nutrient concentration may be an important limitation for growth, while the temperature and irradiation in YS have not reached the limit level to large amount mortality of *U. prolifera* (Figs. 5 and 6). Therefore, the maximum biomass of simulation is bigger than the satellite estimation (Fig. 8).

4.4 Prospects on model development

No technique was identified for the precise quantification of the biomass of floating macroalgae (Sun et al., 2020). Most growth models only considered the environmental factors in a fixed station and disregarded the spatial variation of floating growth. The environmental factors vary greatly at different locations. Base on Lagrangian particle tracking, each particle was considered an independent simulation unit, and the drift velocity and growth rate of each independent particle were obtained according to the natural environmental factors corresponding to the spatial position and time that particles locate. The simulation principle of this model is suitable for the actual situation of massive floating macroalgal blooms, which float and grow across vast regions.

Nutrient eutrophication frequently results in macroalgal blooms in coastal waters (Liu et al., 2013). Despite the difficulty in obtaining the distribution and variations of nutrients, simulations in future studies should incorporate nutrient cycles in the growth of floating macroalgae to improve the coupled model development at a more precise spatiotemporal scale. By coupling with the regional ecosystem or biogeochemical model, this model can also be used to study the consumption of nutrients by the macroalgae blooms and its limitation on the growth of macroalgae. In particular, the model of floating *U. prolifera* could be established as a warning system of green tide disaster forecasting and be an efficient and economical tool for the prevention and management of green tides. Despite being used for the simulation of green tides, this coupled model can also be applied to other large-scale macroalgae disasters that bloom in different parts of the world.

5 Conclusion

A system that coupled the ecological dynamic growth module with the physical drift module for macroalgae was developed to study the spatial and temporal variations of massive floating macroalgal bloom. The dynamic process of growth and drift is achieved by the replication/extinction and Lagrangian tracking of particles. It was applied to the dynamic simulation of YS

green tide blooms that occurred in 2014 and 2015, with environmental drivers from ECS-FVCOM. The simulation results were verified against various observation data and demonstrated reasonable prediction precision. The modeling experiments also suggested that the surface wind played a crucial role in the drifting of *U. prolifera* from local Subei Shoal into regional YS that finally resulted in an annual ecosystem disaster for the adjacent coastal region. The realistic simulation for two years exhibited many uncertainties from natural and human processes during the long duration from early spring to late summer that could potentially lead to extensive prediction bias. However, the short-term simulation, along with the determination of spatial coverage and biomass, in this model proved to be an efficient and robust system for the provision of accurate forecasting of the development of *U. prolifera*.

Although this unique tool for macroalgae prediction was only applied in the simulation of YS green tide, it can potentially be used to study other macroalgae bloom, such as golden tides caused by *Sargassum*, in different regions with sufficient information on the macroalgae physiological relationship with environmental factors and reasonable ocean dynamics model.

Code and data availability

The Fortran code of FMGDM v1.0 is available at https://doi.org/10.5281/zenodo.4607771 (last access: 16 March 2021). The example of the greet tides bloomed in Yellow Sea, China, is available at https://doi.org/10.5281/zenodo.4607829 (last access: 16 March 2021). The ECS-FVCOM forcing data (surface wind, radiations), the ocean bathymetry and the results of ECS-FVCOM (water velocity, temperature and salinity) which are also used as input variables of FMGDM for green tides simulation, the information of seven groups initial particles position, the satellite pictures of green tides in YS, 2014 and 2015, are available at: http://doi.org/10.5281/zenodo.4620534 (last access: 18 March 2021).

Author Contribution

JG proposed and led this model development study. JG and FZ developed the coupled model. DL provided many important suggestions for this study, and key data of *U. prolifera* growth. JG, PD, and CC contributed to the simulation results of ECS-FVCOM systems which is necessary for this research. FZ processed the model outputs and wrote the manuscript with contributions from all co-authors.

Acknowledgments

This research is supported by the National Key R&D Program of China (Grant No. 2016YFA0600903) and the National Natural Science Foundation of China (Grant No. 41776104; 41761144062).

Competing Interests

The authors declare that they have no conflict of interest.

References

Bao, M., Guan, W., Yang, Y., Cao, Z., and Chen, Q.: Drifting trajectories of green algae in the western Yellow Sea during the spring and summer of 2012, Estuarine, Coastal and Shelf Science, 163, 9-16, https://doi.org/10.1016/j.ecss.2015.02.009, 2015.

Brooks, M., Coles, V., Hood, R., and Gower, J.: Factors controlling the seasonal distribution of pelagic Sargassum, Marine Ecology Progress Series, 599, 1-18, https://doi.org/10.3354/meps12646, 2018.

Chen, C., Beardsley, R. C., and Cowles, G.: An unstructured grid, finite-volume coastal ocean model (FVCOM) system. Special issue entitled "Advance in computational oceanography", Oceanography, 19, 78–89, https://doi.org/10.5670/oceanog.2006.92, 2006.

Chen, C., Huang, H., Beardsley, R. C., Liu, H., Xu, Q., and Cowles, G.: A finite volume numerical approach for coastal ocean circulation studies: Comparisons with finite difference models, Journal of Geophysical Research-Oceans, 112, https://doi.org/10.1029/2006JC003485, 2007.

https://doi.org/10.5194/gmd-2021-20
Preprint. Discussion started: 29 March 2021

Geoscientific Model Development Discussions

Chen, C., Liu, H., and Beardsley, R. C.: An unstructured grid, finite-volume, three-dimensional, primitive equations ocean model: Application to coastal ocean and estuaries, Journal of Atmospheric and Oceanic Technology, 20, 159-186, 2003.

Chen, C., Xue, P., Ding, P., Beardsley, R. C., Xu, Q., Mao, X., Gao, G., Qi, J., Li, C., Lin, H., Cowles, G., and Shi, M.: Physical mechanisms for the offshore detachment of the Changjiang Diluted Water in the East China Sea, Journal of Geophysical Research-Oceans, 113, https://doi.org/10.1029/2006JC003994, 2008.

Cui, J., Zhang, J., Huo, Y., Zhou, L., Wu, Q., Chen, L., Yu, K., and He, P.: Adaptability of free-floating green tide algae in the Yellow Sea to variable temperature and light intensity, Marine Pollution Bulletin, 101, 660-666, https://doi.org/10.1016/j.marpolbul.2015.10.033, 2015.

Ding, L. and Luan, R.: The taxonomy, habit and distribution of a green alga Enteromorpha prolifera (Ulvales, Chlorophyta), Oceanol Limnologia Sinica, 40, 68-71, 2009.

Duan, W., Guo, L., Sun, D., Zhu, S., Chen, X., Zhu, W., Xu, T., and Chen, C.: Morphological and molecular characterization of free-floating and attached green macroalgae Ulva spp. in the Yellow Sea of China, Journal of Applied Phycology, 24, 97-108, https://doi.org/10.1007/s10811-011-9654-7, 2011.

Egbert, G. D. and Erofeeva, S. Y.: Efficient inverse modeling of barotropic ocean tides, Journal of Atmospheric and Oceanic technology, 19, 183-204, 2002.

Fan, S., Fu, M., Wang, Z., Zhang, X., Song, W., Li, Y., Liu, G., Shi, X., Wang, X., and Zhu, M.: Temporal variation of green macroalgal assemblage on Porphyra aquaculture rafts in the Subei Shoal, China, Estuarine, Coastal and Shelf Science, 163, 23-28, https://doi.org/10.1016/j.ecss.2015.03.016, 2015.

Garcia, R. A., Fearns, P., Keesing, J. K., and Liu, D.: Quantification of floating macroalgae blooms using the scaled algae index, Journal of Geophysical Research: Oceans, 118, 26-42, https://doi.org/10.1029/2012JC008292, 2013.

Ge, J., Ding, P., Chen, C., Hu, S., Fu, G., and Wu, L.: An integrated East China Sea-Changjiang Estuary model system with aim at resolving multi-scale regional-shelf-estuarine dynamics, Ocean Dynamics, 63, 881-900, http://dx.doi.org/10.1007/s10236-013-0631-3, 2013.

Gower, J. F. R. and King, S. A.: Distribution of floating Sargassum in the Gulf of Mexico and the Atlantic Ocean mapped using MERIS, International Journal of Remote Sensing, 32, 1917-1929, https://doi.org/10.1080/01431161003639660, 2011.

Hu, L., Zeng, K., Hu, C., and He, M.: On the remote estimation of Ulva prolifera areal coverage and biomass, Remote Sensing of Environment, 223, 194-207, https://doi.org/10.1016/j.ecss.2019.106329, 2019.

Keesing, J. K., Liu, D., Fearns, P., and Garcia, R.: Inter- and intra-annual patterns of Ulva prolifera green tides in the Yellow Sea during 2007-2009, their origin and relationship to the expansion of coastal seaweed aquaculture in China, Marine Pollution Bulletin, 62, 1169-1182, https://doi.org/10.1016/j.marpolbul.2011.03.040, 2011.

Lee, J. H., Pang, I. C., Moon, I. J., and Ryu, J. H.: On physical factors that controlled the massive green tide occurrence along the southern coast of the Shandong Peninsula in 2008: A numerical study using a particle-tracking experiment, Journal of Geophysical Research: Oceans, 116, https://doi.org/10.1029/2011JC007512, 2011.

Li, G., Qin, Z., Zhang, J., Lin, Q., Ni, G., Tan, Y., and Zou, D.: Algal density mediates the photosynthetic responses of a marine macroalga Ulva conglobata (Chlorophyta) to temperature and pH changes, Algal Research, 46, 101797, https://doi.org/10.1016/j.algal.2020.101797, 2020a.

Li, J., Song, X., Fan, X., and Yu, Z.: Flocculation of Ulva microscopic propagules using modified clay: a mesocosm experiment, Journal of Oceanology and Limnology, 38, 1283-1291, https://doi.org/10.1007/s00343-020-9348-6, 2020b.

Li, J., Song, X., Zhang, Y., Pan, J., and Yu, Z.: An investigation of the space distribution of Ulva microscopic propagules and ship-based experiment of mitigation using modified clay, Marine Pollution Bulletin, 117, 247-254, https://doi.org/10.1016/j.marpolbul.2017.01.063, 2017.

Liu, D., Keesing, J. K., He, P., Wang, Z., Shi, Y., and Wang, Y.: The world's largest macroalgal bloom in the Yellow Sea, China: Formation and implications, Estuarine, Coastal and Shelf Science, 129, 2-10, https://doi.org/10.1016/j.ecss.2013.05.021, 2013.

Liu, D., Keesing, J. K., Xing, Q., and Shi, P.: World's largest macroalgal bloom caused by expansion of seaweed aquaculture in China, Mar Pollut Bull, 58, 888-895, https://doi.org/10.1016/j.marpolbul.2009.01.013, 2009.

Liu, F., Pang, S. J., Zhao, X. B., and Hu, C. M.: Quantitative, molecular and growth analyses of Ulva microscopic propagules in the coastal sediment of Jiangsu province where green tides initially occurred, Marine Environmental Research, 74, 56-63, https://doi.org/10.1016/j.marenvres.2011.12.004, 2012.

Liu, X., Li, Y., Wang, Z., Zhang, Q., and Cai, X.: Cruise observation of Ulva prolifera bloom in the southern Yellow Sea, China, Estuarine, Coastal and Shelf Science, 163, 17-22, https://doi.org/10.1016/j.ecss.2014.09.014, 2015.

Lovato, T., Ciavatta, S., Brigolin, D., Rubino, A., and Pastres, R.: Modelling dissolved oxygen and benthic algae dynamics in a coastal ecosystem by exploiting real-time monitoring data, Estuarine, Coastal and Shelf Science, 119, 17-30, https://doi.org/10.1016/j.ecss.2012.12.025, 2013.

Luo, M., Liu, F., and Xu, Z.: Growth and nutrient uptake capacity of two co-occurring species, Ulva prolifera and Ulva linza, Aquatic Botany, 100, 18-24, https://doi.org/10.1016/j.aquabot.2012.03.006, 2012.

Lyons, D. A., Arvanitidis, C., Blight, A. J., Chatzinikolaou, E., Guy-Haim, T., Kotta, J., Orav-Kotta, H., Queirós, A. M., Rilov, G., Somerfield, P. J., and Crowe, T. P.: Macroalgal blooms alter community structure and primary productivity in marine ecosystems, Global Change Biology, 20, 2712-2724, https://doi.org/10.1111/gcb.12644, 2014.

Perrot, T., Rossi, N., Ménesguen, A., and Dumas, F.: Modelling green macroalgal blooms on the coasts of Brittany, France to enhance water quality management, Journal of Marine Systems, 132, 38-53, https://doi.org/10.1016/j.jmarsys.2013.12.010, 2014.

Putman, N. F., Goni, G. J., Gramer, L. J., Hu, C., Johns, E. M., Trinanes, J., and Wang, M.: Simulating transport pathways of pelagic Sargassum from the Equatorial Atlantic into the Caribbean Sea, Progress in Oceanography, 165, 205-214, https://doi.org/10.1016/j.pocean.2018.06.009, 2018.

Qi, L., Hu, C., Xing, Q., and Shang, S.: Long-term trend of Ulva prolifera blooms in the western Yellow Sea, Harmful Algae, 58, 35-44, https://doi.org/10.1016/j.hal.2016.07.004, 2016.

Rothäusler, E., Gutow, L., and Thiel, M.: Floating Seaweeds and Their Communities. In: Seaweed Biology: Novel Insights into Ecophysiology, Ecology and Utilization, Wiencke, C. and Bischof, K. (Eds.), Springer Berlin Heidelberg, Berlin, Heidelberg, 2012.

Shi, X., Qi, M., Tang, H., and Han, X.: Spatial and temporal nutrient variations in the Yellow Sea and their effects on Ulva prolifera blooms, Estuarine, Coastal and Shelf Science, 163, 36-43, https://doi.org/10.1016/j.ecss.2015.02.007, 2015.

Smetacek, V. and Zingone, A.: Green and golden seaweed tides on the rise, Nature, 504, 84-88, https://doi.org/10.1038/nature12860, 2013.

Son, Y. B., Min, J.-E., and Ryu, J.-H.: Detecting Massive Green Algae (Ulva prolifera) Blooms in the Yellow Sea and East China Sea using Geostationary Ocean Color Imager (GOCI) Data, Ocean Science Journal, 47, 359-375, https://doi.org/10.1007/s12601-012-0034-2, 2012.

https://doi.org/10.5194/gmd-2021-20
Preprint. Discussion started: 29 March 2021

Geoscientific Model Development Discussions

Song, W., Peng, K., Xiao, J., Li, Y., Wang, Z., Liu, X., Fu, M., Fan, S., Zhu, M., and Li, R.: Effects of temperature on the germination of green algae micro-propagules in coastal waters of the Subei Shoal, China, Estuarine, Coastal and Shelf Science, 163, 63-68, https://doi.org/10.1016/j.ecss.2014.08.007, 2015.

Sun, K., Ren, J. S., Bai, T., Zhang, J., Liu, Q., Wu, W., Zhao, Y., and Liu, Y.: A dynamic growth model of Ulva prolifera: Application in quantifying the biomass of green tides in the Yellow Sea, China, Ecological Modelling, 428, 109072, https://doi.org/10.1016/j.ecolmodel.2020.109072, 2020.

Teichberg, M., Fox, S. E., Olsen, Y. S., Valiela, I., Martinetto, P., Iribarne, O., Muto, E. Y., Petti, M. A. V., Corbisier, T. N., Soto-JimÉNez, M., PÁEz-Osuna, F., Castro, P., Freitas, H., Zitelli, A., Cardinaletti, M., and Tagliapietra, D.: Eutrophication and macroalgal blooms in temperate and tropical coastal waters: nutrient enrichment experiments with Ulva spp, Global Change Biology, 16, 2624-2637, https://doi.org/10.1111/j.1365-2486.2009.02108.x, 2010.

Wang, C., Su, R., Guo, L., Yang, B., Zhang, Y., Zhang, L., Xu, H., Shi, W., and Wei, L.: Nutrient absorption by Ulva prolifera and the growth mechanism leading to green-tides, Estuarine, Coastal and Shelf Science, 227, https://doi.org/10.1016/j.ecss.2019.106329, 2019.

Wang, M. and Hu, C.: Mapping and quantifying Sargassum distribution and coverage in the Central West Atlantic using MODIS observations, Remote Sensing of Environment, 183, 350-367, https://doi.org/10.1016/j.rse.2016.04.019, 2016.

Wang, Z., Fu, M., Xiao, J., Zhang, X., and Song, W.: Progress on the study of the Yellow Sea green tides caused by Ulva prolifera., Acta Oceanologica Sinica, 40, 1-13, https://doi.org/10.3969/j.issn.0253-4193.2018.02.001, 2018.

Xiao, J., Wang, Z., Song, H., Fan, S., Yuan, C., Fu, M., Miao, X., Zhang, X., Su, R., and Hu, C.: An anomalous bi-macroalgal bloom caused by Ulva and Sargassum seaweeds during spring to summer of 2017 in the western Yellow Sea, China, Harmful Algae, 93, 101760, https://doi.org/10.1016/j.hal.2020.101760, 2020.

Xiao, J., Zhang, X., Gao, C., Jiang, M., Li, R., Wang, Z., Li, Y., Fan, S., and Zhang, X.: Effect of temperature, salinity and irradiance on growth and photosynthesis of Ulva prolifera, Acta Oceanologica Sinica, 35, 114-121, https://doi.org/10.1007/s13131-016-0891-0, 2016.

Xu, Q., Zhang, H., Ju, L., and Chen, M.: Interannual variability of Ulva prolifera blooms in the Yellow Sea, International Journal of Remote Sensing, 35, 4099-4113, https://doi.org/10.1080/01431161.2014.916052, 2014.

Ye, N., Zhang, X., Mao, Y., Liang, C., Xu, D., Zou, J., Zhuang, Z., and Wang, Q.: 'Green tides' are overwhelming the coastline of our blue planet: taking the world's largest example, Ecological Research, 26, 477-485, https://doi.org/10.1007/s11284-011-0821-8, 2011.

Yuanzi, H., Liang, H., Hailong, W., Jianheng, Z., Jianjun, C., Xiwen, H., Kefeng, Y., Honghua, S., Peimin, H., and Dewen, D.: Abundance and distribution of Ulva microscopic propagules associated with a green tide in the southern coast of the Yellow Sea, Harmful Algae, 39, 357-364, https://doi.org/10.1016/j.hal.2014.09.008, 2014.

Zhang, X., Wang, H., Mao, Y., Liang, C., Zhuang, Z., Wang, Q., and Ye, N.: Somatic cells serve as a potential propagule bank of Enteromorpha prolifera forming a green tide in the Yellow Sea, China, Journal of Applied Phycology, 22, 173-180, https://doi.org/10.1007/s10811-009-9437-6, 2009.

Zhou, M., Liu, D., Anderson, D. M., and Valiela, I.: Introduction to the Special Issue on green tides in the Yellow Sea, Estuarine, Coastal and Shelf Science, 163, 3-8, https://doi.org/10.1016/j.ecss.2015.06.023, 2015.

Zhu, J., Yu, Z., He, L., Cao, X., Liu, S., and Song, X.: Molecular Mechanism of Modified Clay Controlling the Brown Tide Organism Aureococcus anophagefferens Revealed by Transcriptome Analysis, Environmental Science & Technology, 52, 7006-7014, https://doi.org/10.1021/acs.est.7b05172, 2018.